Application of infrared reflecting (IRR) coverglass on multijunction III-V solar cells

Hojun Yoon, David E. Joslin, Daniel C. Law, Dmitri Krut, Richard R. King,
P. Vijayakumar, David Peterson, Jim Hanley, and Nasser H. Karam

Spectrolab, Inc., 12500 Gladstone Avenue, Sylmar, CA 91342, USA

ABSTRACT

It is well known that the Ge subcell in multijunction GaInP/GaAs/Ge based solar cells produces a significantly higher photogenerated current (nearly 2x) than the other two subcells connected in series. The excess current is converted into heat, and as a result, increases the cell operating temperature. Because the solar cell efficiency decreases with higher temperatures, it is desirable to maintain a lower cell operating temperature. This can be achieved by rejecting a part of the incident sunlight that would otherwise be absorbed and converted into heat by the Ge subcell. For many space applications, coverglass incorporated with infrared reflecting (IRR) coatings can be applied to these solar cells for the purpose of lowering the cell operating temperature and/or improving the power output from the solar arrays. Achieving higher power output requires an appropriate IRR coating design that carefully balances the reduction in the cell absorptance against the Ge subcell current output. In this paper, this key issue is discussed. Also, preliminary IRR coating designs have been evaluated by applying them on high efficiency 3-junction solar cells, and the performance data are used to help predict optimal designs.

INTRODUCTION

Space solar cell coverglasses are typically coated with a simple anti-reflective (AR) coating such as MgF_2, and provides high optical transmission across the entire solar cell response wavelengths and beyond. By reflecting a portion of the incident sunlight that is outside of the cell response range, the absorptance of the cell assembly and consequently the cell operating temperature, can be reduced (provided the emittance remains constant). Lower cell operating temperature on orbit can result in increased power output from the solar arrays. Reflecting selective wavelength ranges can be achieved by the use of appropriate coating designs on the coverglass.

The work presented in this paper is an extension of the earlier work initiated by Moy [1] who recognized the useful benefits of employing infrared reflecting (IRR) coverglass designs to 3-junction GaInP/GaAs/Ge based solar cells. The earlier work involved optical and thermal modeling, as well as fabrication and characterization of several IRR coated coverglass samples from coating vendors Sonoma Photonics and MLD Technologies. The key issue relates to whether useful temperature reduction and/or performance gains can be obtained by placing the IRR cut-on point inside the Ge response range, which extends out to 1800 nm. This work is unique in that it applies to 3-junction solar cells (i.e., GaInP/GaAs/Ge where Ge is an active subcell). Indeed, the potential benefits of this general concept have long been recognized, but on various single-junction (Si and GaAs) space cells [2-5], where the selection of the IRR cut-on point is fairly straightforward.

This paper is organized as follows:
(1) Review of the solar spectrum and the Ge subcell response;
(2) Analysis of the cell performance tradeoff between the gain due to lower temperature (absorptance) and the loss due to a reduction in the Ge subcell photocurrent;
(3) Evaluation of preliminary IRR-coated coverglass designs and their impact on the Ge subcell performance.

The analysis in this study pertains to beginning of life conditions only. The end of life performance, particularly of the Ge subcell [6], and its potential influence on this analysis is considered for future work.

SOLAR SPECTRUM AND Ge SUBCELL RESPONSE

Figure 1 shows the AM0 spectrum with approximate partitions for the 3J GaInP/GaAs/Ge solar cell. Note that the response extends out to 1800 nm due to the Ge subcell, far beyond the response ranges for Si (~1100 nm) and GaAs (~890 nm). The inset pie chart in the figure shows the approximate distribution of the photogenerated currents for the three subcells. Note that the Ge subcell produces nearly two times more current than the other 2 subcells in the 3J device.
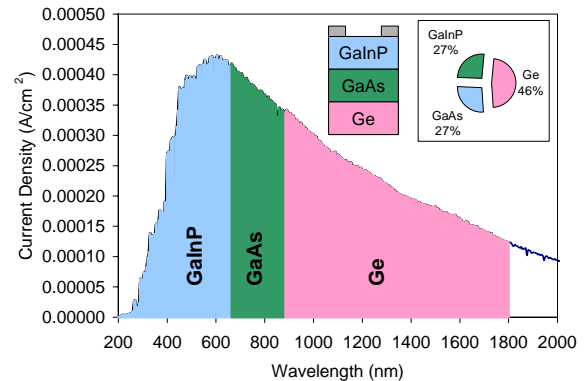

Fig. 1. AM0 spectrum with approximate partitions for the 3J GaInP/GaAs/Ge solar cell. Inset pie chart shows the approximate distribution of the photogenerated currents for the three subcells.

If the IRR coating for the 3J device coverglass is designed using the same approach as was done for Si and GaAs cells, it would start reflecting near the Ge band edge of 1800 nm. This design would not significantly affect the absorptance of the cell assembly and hence no practical benefits are expected. However, since the Ge subcell pro-

duces excess current, one may actually shift the IRR cut-on wavelength within the Ge response range.

Figure 2 provides an external quantum efficiency (EQE) curve of a Ge subcell in a typical high efficiency 3J solar cell, along with the AM0 spectrum and the cumulative current expected from the Ge subcell as a function of wavelength. When integrated over the entire response range (up to 1800 nm), the current density is ~30 mA/cm^2. In comparison, the operating short circuit current density of a typical 3J GaInP/GaAs/Ge cell is ~17 mA/cm^2. This value, as can be observed from Fig. 2, is achieved by the Ge subcell at a wavelength of ~1250 nm. Although one might conclude that this would be an appropriate IRR cut-on wavelength that will maximize the performance, it is not the case because the Ge subcell influences the overall 3J device performance under different illumination conditions. This key point is addressed in the next section.
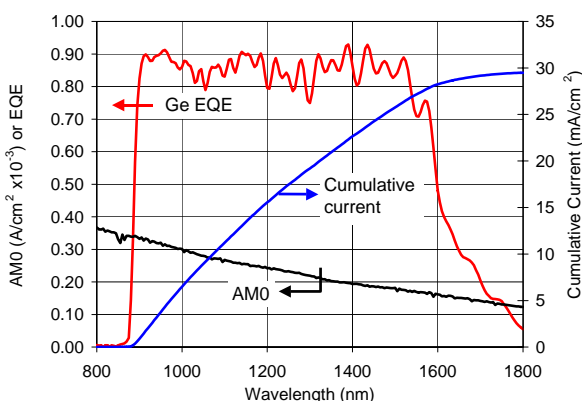

Fig. 2. EQE of a Ge subcell in a typical high efficiency 3J solar cell. Also plotted are the AM0 spectrum and the cumulative current expected from the Ge subcell as a function of wavelength.

PERFORMANCE TRADE-OFF

Effect of temperature on 3J cell performance

The performance gain expected from the IRR coverglass can be estimated from the temperature coefficients of 3J cells, namely for V_{mp} and J_{mp}. Table I provides temperature coefficients (15-75ºC, Beginning of Life) of V_{mp} and J_{mp} for typical high efficiency GaInP/GaAs/Ge based 3J solar cells. There is a competing effect between the current and voltage of the solar cell as a function of temperature; however, the net effect is that the efficiency (power output) drops as temperature increases, as the voltage component dominates the behavior. Therefore, by using IRR coverglass to maintain a lower cell temperature, the overall power output can be increased (by means of voltage enhancement).

Table I. Temperature coefficients (15-75ºC, Beginning of Life) of V_{mp} and J_{mp} for typical high efficiency GaInP/GaAs/Ge based 3J solar cells.

Parameter	Value
V_{mp}	~ –6.5 mV/ºC
J_{mp}	1–7 μA/cm^2/ºC

Effect of reduced photogenerated current on Ge subcell performance

Fig. 3 addresses the key performance loss mechanism that needs to be considered for choosing the appropriate IRR design. It shows schematic light IV curves of a Ge subcell in a typical 3J device (1) for a standard 1-sun AM0 condition and (2) for a reduced Ge photogenerated current condition, as will be the case when an IRR coverglass is used on a 3J device. Because the 3 subcells in a 3J stack are in series, the current flowing through the circuit is limited by the lowest current producing subcell. Condition (2) is a case where the Ge subcell is still producing more current than the other 2 subcells, but simply less than in condition (1). When condition (2) occurs, the voltage of the 3J stack would be slightly lower because of the relatively poor fill factor of the Ge subcell (an example at current at load is indicated in Fig.3).
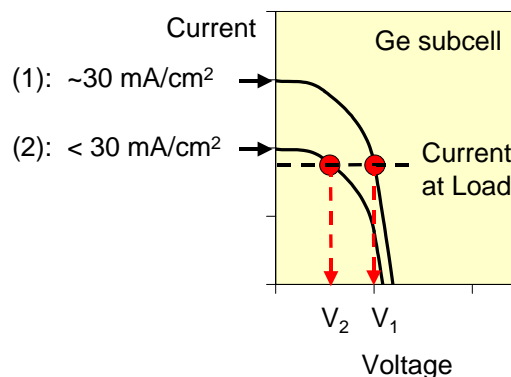

Fig. 3. Schematic light IV curves of a Ge subcell (1) for typical 1-sun AM0 condition and (2) for a reduced Ge photogenerated current condition in a 3J stack. For condition (2), the voltage of the 3J stack would be lower by (V_1-V_2) near the current at load point.

Final trade-off analysis

The final trade-off analysis can be made by knowing the relationship between the absorptance (α) and the temperature of the cell assembly. A reasonable assumption, and a general rule of thumb is that

Case 1: Δ of 1 "α point" $\approx \Delta$ **1ºC**.

This implies that a 10-point reduction in α would be equivalent to a 10ºC reduction in temperature. However, extensive thermal modeling [1] suggests that

Case 2: Δ of 1 "α point" $\approx \Delta$ **1.5ºC**

is a likely condition for a typical GEO (geosynchronous earth orbit) spacecraft, meaning that a 10-point reduction in α would lower the temperature by 15ºC. Clearly this value would vary somewhat (in fact, >1.5ºC per α in many cases according to thermal modeling), depending on the nature of the spacecraft and its operating condition. However, the

following trade-off analysis will consider the above two cases for illustrative purposes.

It is also noted that in this analysis, the IRR cut-on is assumed to be ideal, – that is, the transmission is zero beyond the cut-on wavelength. Actual IRR optical performance, as will be seen later, has a small amount of transmission beyond the IRR cut-on wavelength.

Figure 4 and 5 summarize the trade-off results for Case 1 and 2, respectively. For the temperature effect, the voltage is only considered because it is the dominating parameter. The competing current component is small and can be taken into account separately. In the figures, voltage gain or loss from the Ge subcell is plotted against the IRR cut-on wavelength. The dashed lines represent the 2 competing effects described earlier in this section, and the solid line is the combined total. In each case, the upper dashed line is the voltage gain expected due to the temperature effect, while the lower dashed line is the voltage loss expected due to the impact of the Ge subcell fill factor on the 3J devices.
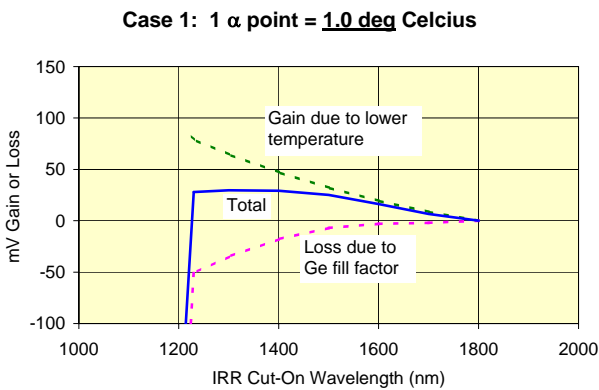
Case 1: 1 α point = <u>1.0 deg</u> Celcius

Fig. 4. Summary of the IRR performance trade-off analysis for Case 1 where 1α point = 1°C is assumed. Maximum voltage gain is expected for IRR cut-on wavelength of ~1350 nm. The sharp drop-off near 1200 nm occurs because below this value, the Ge subcell becomes current limiting in a 3J device.
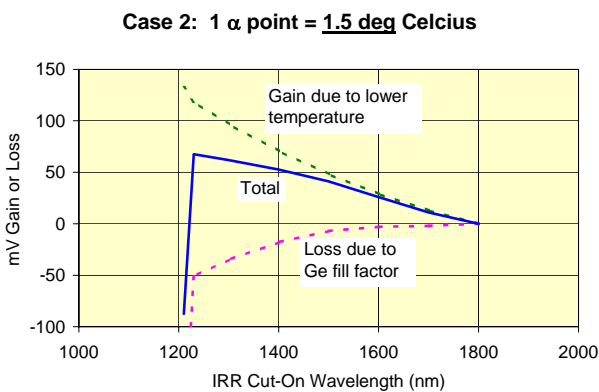
Case 2: 1 α point = <u>1.5 deg</u> Celcius

Fig. 5. Summary of the IRR performance trade-off analysis for Case 2 where 1α point = 1.5°C is assumed. The sharp drop-off near 1200 nm occurs because below this value, the Ge subcell becomes current limiting in a 3J device.

Referring to the upper dashed line in Figure 4, as the IRR cut-on starts to move in from 1800 nm (Ge band edge), the absorptance and hence the cell temperature decreases. The change in absorptance is simply calculated from the energy content of the AM0 sun that is available up to the Ge response range. For example, if the IRR cut-on is at 1400 nm, the absorptance (α) is expected to decrease by ~10 points. The voltage gain is then calculated in a straightforward manner using the relationship between the α and the temperature, combined with the 3J temperature coefficient (Table I) for the voltage (V_{mp} in this case).

In contrast, for the lower dashed line in Figure 4, as the IRR cut-on starts to move in from 1800 nm, the photogenerated current density in the Ge subcell starts to decrease, and because of the relatively poor fill factor of the Ge subcell, the voltage of the overall 3J device is lowered (this was described in Figure 3). The light IV behavior of the Ge subcell was modeled as a function of different photogenerated current density, and this allowed the determination of the relationship between the Ge subcell current density and the voltage change (near the 3J load point) as indicated in Figure 3. As should be the case, this effect is independent of the assumptions made for Case 1 and 2, so that the lower dashed lines in Figure 4 and 5 are identical.

The sharp drop-off near 1200 nm in both Figure 4 and 5 occurs because below this value, the Ge subcell becomes current limiting in a 3J device, and near the load point, there would essentially be no voltage contribution from the Ge subcell. Because of this effect, it will be important to ensure that this condition will not occur, i.e., the IRR cut-on point should have some "margin" in its design.

In summary, for Case 1, a maximum voltage gain of ~30 mV is expected for IRR cut-on wavelength of ~1350 nm. This represents an increase of ~1.3% in power, which would be adjusted to ~1.0% after accounting for the slight current reduction due to lower temperature. For Case 2, the maximum point does not occur before reaching the critical wavelength below which the Ge subcell becomes current limiting. In this case, by choosing a cut-on point of 1300 nm, which is reasonably away (~70 nm) from the critical wavelength, a voltage gain of ~60 mV is expected, or a 2.6% increase in power. This value would be adjusted to ~2.2% after accounting for the slight current reduction due to lower temperature.

EVALUATION OF PRELIMINARY IRR COVER-GLASS DESIGNS

Figure 6 plots the measured transmission curves of a standard space coverglass and two (A, B) variations of IRR coating designs. The A and B designs were measured to have IRR cut-on of ~1275 and 1385 nm, respectively. The measured α values for A and B were 0.77 and 0.81, respectively. While the α for space 3J cells with conventional coverglass is ~0.92, the measured α for the various IRR coverglass designs in this study ranged from 0.75-0.86.

Figure 7 compares the measured EQE curves of a Ge subcell illustrating the effect of the IRR coverglass (design B in Figure 6). Note that the IRR coverglass has effectively narrowed the Ge response range to <1400 nm.

The integrated current density (for AM0) values for without and with the IRR coverglass are 31.5 and 23.4 mA/cm^2, respectively.
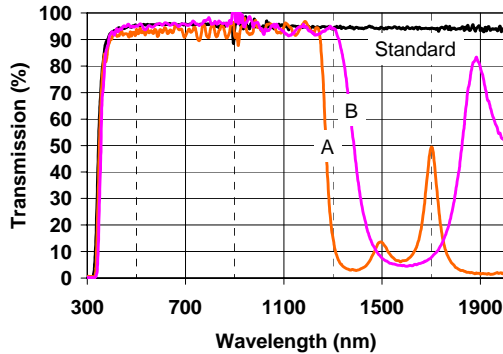

Fig. 6. Measured transmission curves of a standard space coverglass and two (A, B) variations of IRR coating designs.
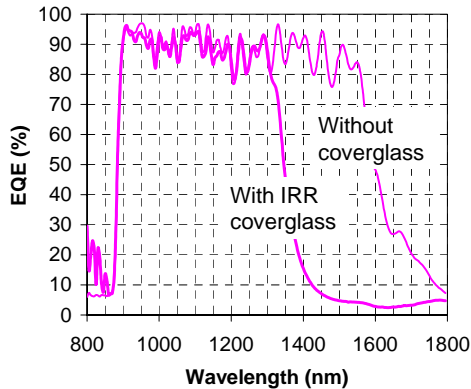

Fig. 7. Comparison of measured EQE curves of a Ge subcell illustrating the effect of one particular IRR coverglass.

The data shown in Fig. 6 and 7 demonstrate the optical characteristics of the IRR coating as well as the key impact that it has on the Ge subcell response. The absorptance measured on complete 3J cell assemblies verifies the effectiveness of the IRR coating and its ability to reduce the on-orbit cell temperature and increase the cell power output.

SUMMARY

Key issues related to the application of IRR coverglass on multijunction III-V solar cells (specifically on 3J GaInP/GaAs/Ge based cells) have been reviewed. Useful reduction in the absorptance of the cell assembly is primarily achieved by reflecting the IR content of the incident solar spectrum that is used by the Ge subcell. However, some of the temperature benefit is offset by the character of the light IV response of the Ge subcell as the photogenerated current is reduced in that subcell. Several preliminary IRR coating designs have been evaluated on high efficiency 3J solar cells. Data indicate that important on-orbit solar array performance gains can be obtained by applying the appropriate IRR coverglass design to today's state-of-the-art 3J III-V solar cells.

REFERENCES

[1] Robert Moy, US Patent Application Publication No. US2005/0103374A1.

[2] W.T. Beauchamp, T.T. Hart, and M.L. Sanders, "Blue/Red Reflecting Solar Cell covers for GaAs Cells", Proceedings of the 23rd IEEE PVSC, May 1993, pp. 1487-90.

[3] K. Mullaney, G.M. Jones, C.A. Kitchen, and D.P. Jones, "Infra-Red Reflective Coverglasses: The Next Generation", Proceedings of the 23rd IEEE PVSC, May 1993, pp. 1363-68.

[4] W.T. Beauchamp, B. McLean, and M. Larro, "Qualification Test Results for Blue-Red Reflecting Solar Cell Covers and Other New Products for the Solar Power Market", Proceedings of the 24th IEEE PVSC and WCPEC-1, Dec. 1994, pp. 2062-65.

[5] G. Jones, K. Mullaney, C. Kitchen, and J.C. Larue, "The Infra Red Reflecting Coverglass for Silicon & GaAs Solar Cells Used in Near Earth & Geostationary Orbits", Proceedings of the 24th IEEE PVSC and WCPEC-1, Dec. 1994, pp. 2054-57.

[6] Hojun Yoon, K.M. Edmondson, G.S. Kinsey, R.R. King, P. Hebert, R.K. Ahrenkiel, B.T. Cavicchi, and N.H. Karam, "Minority carrier lifetime and radiation damage coefficients of germanium", Proceedings of the 31st IEEE PVSC, Jan. 2005, pp. 842–45.